Spatio-temporal dynamics of microbial population under nutrient-limiting conditions

Michael Chapwanya*, Phindile Dumani

Department of Mathematics & Applied Mathematics, University of Pretoria, Pretoria 0002, South Africa

A B S T R A C T

The physiological structure of microbial communities in natural environments is typically a response to changes in internal and external conditions. External conditions may include the availability of nutrients, and the presence of inhibiting or toxic substances while internal conditions may include cell to cell interactions. In this paper, we present and investigate a spatio-temporal bacterioplankton-nutrient interaction model that takes into account the quiescent stage. First, we investigate the temporal submodel to establish conditions under which microbial population oscillations may occur. Furthermore, we establish the existence of traveling wavefronts for the proposed reaction-diffusion model. A qualitative study of the proposed numerical scheme is presented and simulations are provided to support our theoretical results.

Keywords:
Microbial quiescence
Bacterioplankton
Traveling waves
Nonstandard finite difference

1. Introduction

Microbial populations can be found almost everywhere and anywhere. They play a crucial role in ecological, environmental, as well as industrial processes. Regardless of their preponderance contribution in biology to sustain life on the planet, there is minimal knowledge about microbial biology. For instance, one small insect can contain thousands of microbial organisms of many different species. Despite these limitations, robust experimental work making use of axenic culture methods (among others) have been conducted over the last several decades. Such studies have provided basic knowledge and understanding of the dynamics and development of microbiology. However, the dynamics or interactions observed using such methods are unrealistic. In reality, there is a wide variety of microbial species and complex interactions that pure culture methods do not capture, see for example [1] for a review.

In many populations, not all individuals are actively growing and proliferating but some are in a quiescent state [2]. In the case of microorganisms, they have the ability to resist stressors such as antibiotics, unfavourable temperature and desiccation by entering a state of low metabolic activity, i.e., dormancy, see for example [3,4] and the literature therein. However, it has also been found that microbes may also be dormant under natural environmental conditions. Microbial populations in a state of dormancy are neither dead nor active which allows for them to persist under various environmental challenges [5,6], a strategy of great importance, for example, in medical studies. For instance, spores are highly resistant to disinfectants as a result, they stay dormant in wounds for periods longer than the applied disinfectant. This normally accounts for the recurrence of infections. A distinct character of microbes in a dormant state is the ability to transition between an active state and a relatively inactive but live state and thereafter be reactivated again.

* Corresponding author.
E-mail address: m.chapwanya@up.ac.za (M. Chapwanya).

This work includes and focuses on microbial quiescence/activity as a direct response to either rate-limiting nutrient levels, or a direct consequence of paracrine signalling from other cells. Paracrine signaling in bacterial populations is where some cells produce a signal to which only certain target cells respond [7,8]. For example, biofilm formation in Bacillus involves two centrally important signaling molecules, ComX and surfactin where ComX triggers the production of surfactin. In turn, surfactin causes a subpopulation of cells to produce an extracellular matrix (or a biofilm) [8]. That is, bacteria use diverse small molecules for extra-and intracellular signaling. They have an ability to scan molecule mixtures of small-scale to retrieve information about both their extracellular environment and their intracellular physiological status, and depending on the information, they continuously interpret their circumstances and react quickly to changes [7].

Quiescence is a very important phenomenon, especially in ecology and population biology, particularly when populations oscillate. In population dynamics, it is not unusual for a population to reach very low levels; too low that in reality the population would go extinct [9,10]. For example, the phenomenon is observed in the study of the recurrent fox rabies outbreaks in [11]. Models of the immune response commonly exhibit such dynamics of populations of self-replicating antigen and specific antibodies due to the antigen-stimulated antibody production and the antagonistic antibody-antigen interaction [12,13]. Population models with delay as well as those that exhibit boom-and-bust dynamics and plankton blooms show such features. Often such blooms are viewed as a signal of impending eutrophication, indicating that ecosystem balance is lost and that nutrients may have reached unacceptably high levels, or high enough to support massive bloom formations [14]. However, the above mentioned studies and majority found literature (for example, the work found in [14–16] and references therein) focus on models representing the interaction between an active population and its rate-limiting nutrient. Thus, our interest lies in the interaction between a population of autotrophic organisms and its rate-limiting nutrient, as well as their activity as a direct response to either rate-limiting nutrient level changes or consequence of paracrine signalling.

Various experiments have been done using different experimental assay methods. Observed results are used to inform mathematical modellers in designing models that better predict and give informed knowledge of bacteria behaviour [17]. Environment, as well as conditions in nature vary from those of the laboratories [4]. Under a variety of experimental conditions, diverse subtypes of bacteria aggregate forming temporary macroscopic patterns that are both complex and unique [18]. Explaining formation of these patterns solely by experiments is not an easy task but it is possible with the prediction power of mathematical models formulated based on the known biology [19]. Mathematical models formulated with the aim to explain phytoplankton bloom are available in the literature. See for example the work [20,21]. Using nonautonomous ordinary differential equations, the authors hypothesised that temperature variations are responsible for the observed pattern.

Environmental heterogeneity has been observed to contribute to patchiness in oceanic plankton populations. Biological interactions involving phytoplankton populations can result in similar patterns. Formation of spontaneous patterns even in homogeneous environments is a phenomenon that is a trait of reaction-diffusion equations employed to model similar systems, see for example [22], and more recent work in [20,21]. Bacterioplankton are bacteria and archaea, which play an important role in remineralising organic material in lakes and oceans. Many phytoplankton are also bacterioplankton. Plankton population movement is subject to other factors such as currents and turbulent lateral diffusion, [23]. In this work, we consider a general phytoplankton population where b denotes active population density, a the corresponding dormant population density and c the rate-limiting nutrient concentration. The novelty of this work is threefold. First, motivated by the existing literature, we propose a reaction-diffusion mathematical model incorporating dormant and active microbial population. Using the reduced temporal model, we address whether the observed boom-and-bust dynamics (population oscillations) are a response to rate-limiting nutrient concentration levels or a result of paracrine signalling. Furthermore, we will establish conditions for existence of traveling waves describing the rate of spread of the phytoplankton population.

The remainder of this paper is organized as follows. We begin in Section 2 by proposing a nutrient-bacterioplankton reaction diffusion system. The modeling assumptions are included in this section. A uniform steady state model is investigated in Section 3 with the aim to establish if population oscillations are a response to the rate-limiting nutrient concentration levels or a result of paracrine signalling. The existence of traveling waves is established in Section 4 with the numerical results provided in Section 5. We conclude in Section 6.

2. Model formulation

We begin by describing the model kinetics in detail. Autotrophs are organisms that are capable of producing their own food by using various inorganic components like water, sunlight, air, and other chemical substances. They convert an abiotic source of energy into energy stored in organic compounds, which can be used by other organisms, e.g., heterotrophs [24]. Phytoplankton are the autotrophic components of the plankton community and a key part of ocean and freshwater ecosystems. We denote by $a(t)$ and $b(t)$ the density of inactive and active autotrophic microorganisms, respectively, and $c(t)$ the concentration of the limiting nutrient. The growth rate of active microorganisms is given by

$$\frac{1}{b}\frac{db}{dt} = \mu_m f(c),$$

where μ_m is the utilisation constant with $f(c)$ the response function which may take different forms [10,25]. The simplest form will be a linear function, $f(c) = c$, with possibility of nonlinear behavior as expressed by the Monod law, $f(c) = \dfrac{c}{k_c + c}$, [25]. To quote the authors in [10], the choice has *cosmetic effect* on the dynamics of the model, hence, we assume $f(c)$ satisfies the following general hypothesis

$\mathcal{G}$: $f : \mathbb{R}_+ \to [0, +\infty)$ is C^1 and $f'(c) \geq 0$ for all c.

For mathematical convenience, we further assume $f(c) = ch(c)$ which satisfies hypothesis $\mathcal{G}$. In the absence of any other dynamics, the efficiency of conversion of $c(t)$ into $b(t)$ is measured by the yield constant Y, that is

$$Y = -\frac{db/dt}{dc/dt},$$

with $c(t)$ assumed to be the only limiting nutrient. See for example [26]. We hypothesise that microorganisms may enter a quiescent phase in which they need resuscitation for proliferation as opposed to active ones [10,25]. Consequently, only active microbes contribute towards biomass growth [6]. The transformation of $a(t)$ to $b(t)$ (awakening), takes place at rate s^*, and hibernation, i.e., from $b(t)$ to $a(t)$ takes place at the rate r^*. We also introduce hibernation and reawakening functions, $q(V)$ and $p(U)$, respectively, each of them $\in (0, 1)$. The variables V and U describe the dependence of switching, and these variables can either be $b(t)$ or $c(t)$. For example, if both processes are nutrient dependent, then p and q will be functions of $c(t)$. In particular, assuming a switch dependent on the nutrient suggests that q and p are increasing and decreasing functions of c, respectively; with q and p as functions of b if the switch is due to paracrine signalling. This, of course, as argued in [10], may need further investigation when the reactivation of dormant cells is controlled by microbial density. These biological processes lead to the following equations governing the dynamics of the active and dormant microorganisms

$$\begin{cases} \dfrac{da}{dt} = r^* q(V) b - s^* p(U) a - \mu a, \\ \dfrac{db}{dt} = Y \mu_m f(c) b - \mu b - r^* q(V) b + s^* p(U) a, \end{cases} \tag{2.1}$$

where we have assumed a microbial natural mortality rate μ. The switch functions are assumed to be monotonic and saturate. In particular, we have

$\mathcal{H}_1$: $p : \mathbb{R}_+ \to (0, 1]$ is C^1, $p'(U) \geq 0$ for all U and $\lim\limits_{U \to \infty} p(U) = 1$,
$\mathcal{H}_2$: $q : \mathbb{R}_+ \to (0, 1]$ is C^1, $q'(V) \leq 0$ for all V and $\lim\limits_{V \to \infty} q(V) = 0$.

The active microorganisms are assumed to produce a nutrient that can also be used by other microorganisms at the rate $\gamma g(b)$. In addition, we assume a natural degradation of the nutrient at the rate ν. The nutrient dynamics are governed by the following equation

$$\frac{dc}{dt} = \gamma g(b) - \nu b - \mu_m f(c) b,$$

where $g(b)$ is the production function that includes input from both external sources and active biomass, hence we assume $g(b)$ satisfies the following conditions: $g(b) > 0$, $g'(b) > 0$, $g''(b) \leq 0$ for all $b \geq 0$. For further details, readers can consult for example, the work [20,21] and the references therein.

Allowing for the random movement of active population and the nutrient with rates D_b and D_c, respectively, we propose a multi-dimensional nonlinear reaction-diffusion partial differential equation describing the key properties of the population in response to availability and sufficiency of the nutrient. Let $x \in \Omega \subset \mathbb{R}^\rho$, $(\rho \geq 1)$ be a simply connected bounded domain and $\partial\Omega$, the surface boundary enclosing Ω. We let $a(x, t) \geq 0$, $b(x, t) \geq 0$ and $c(x, t) \geq 0$ be the density of dormant population, density of active population and the concentration of the nutrient, respectively. Following the above mentioned biological processes, and in particular, motivated by existing literature [10,27,28], we propose the following generalised diffusive model

$$\begin{cases} \dfrac{\partial a}{\partial t} = r^* q(V) b - s^* p(U) a - \mu a, \\ \dfrac{\partial b}{\partial t} = Y \mu_m f(c) b - \mu b - r^* q(V) b + s^* p(U) a + D_b \nabla^2 b, \qquad x \in \Omega, t > 0. \\ \dfrac{\partial c}{\partial t} = \gamma g(b) - \nu c - \mu_m f(c) b + D_c \nabla^2 c, \end{cases} \tag{2.2}$$

The model is rendered dimensionless by choosing the following scales:

$$a \sim \frac{\mu}{\mu_m}, \quad b \sim \frac{\mu}{\mu_m}, \quad c \sim \frac{\mu}{\mu_m Y}, \quad x \sim \sqrt{\frac{D_b}{\mu}}, \quad t \sim \frac{1}{\mu}.$$

The corresponding dimensionless system takes the form

$$\begin{cases} \dfrac{\partial a}{\partial t} = r q(V) b - s p(U) a - a, \\ \dfrac{\partial b}{\partial t} = (f(c) - 1) b - r q(V) b + s p(U) a + \nabla^2 b, \qquad x \in \Omega, t > 0, \\ \dfrac{\partial c}{\partial t} = \alpha(\beta g(b) - c) - b f(c) + d_c \nabla^2 c, \end{cases} \tag{2.3}$$

where $d_c = \frac{D_c}{D_b}$, $\beta = \frac{\gamma \mu_m Y}{\nu^2}$, $r = \frac{r^*}{\mu}$, $s = \frac{s^*}{\mu}$ and $\alpha = \frac{\nu}{\mu}$. System (2.3) is degenerate in the sense that the inactive population does not diffuse. In the next section, we investigate the temporal model dynamics with the aim to set the stage for the analysis of a monostable wavefront connecting the model equilibria. The system is appended by the following boundary conditions

$$\frac{\partial a}{\partial n} = 0, \quad \frac{\partial b}{\partial n} = 0, \quad \frac{\partial c}{\partial n} = 0, \quad x \in \partial\Omega, \tag{2.4}$$

where $\partial/\partial n$ denotes the derivative with respect to the outer normal of $\partial\Omega$. The initial conditions are $a(x,0) = a^0(x) \geq 0$, $b(x,0) = b^0(x) \geq 0$, $c(x,0) = c^0(x) \geq 0$.

3. Temporal model dynamics

Several spatially independent differential models of microbial quiescence are documented in the literature, see [4,10,27–29], to name a few. The authors in [28] proposed a resource-based model on microbial quiescence with smooth transition functions. In [27], the authors assumed the transition functions depend on the rate-limiting nutrient since cells' metabolism changes according to the nutrient levels. For mathematical convenience, they assumed that there are threshold values for both switch functions: the reawakening rate is non-decreasing for the nutrient greater than some threshold value, and the hibernation rate is non-increasing for the nutrient less than some threshold value. Here, our non-diffusive model takes the form

$$\begin{cases} \dfrac{da}{dt} = rq(V)b - sp(U)a - a, \\ \dfrac{db}{dt} = (ch(c) - 1)b - rq(V)b + sp(U)a, \\ \dfrac{dc}{dt} = \alpha(\beta g(b) - c) - bch(c), \end{cases} \qquad t > 0, \tag{3.1}$$

with initial conditions $a(0) = a_0 \geq 0$, $b(0) = b_0 \geq 0$ and $c(0) = c_0 \geq 0$. Adding all the equations in (3.1), with $\omega = a + b + c$, we obtain

$$\tfrac{d\omega}{dt} = \alpha\beta g(b) - a - b - \alpha c \leq \kappa - \alpha_m(a + b + c) = \kappa - \alpha_m\omega, \tag{3.2}$$

where $\alpha_m = \min\{1, \alpha\}$ and $\kappa = \alpha\beta \max_{b\geq 0}[g(b)]$ with $g(b)$ assumed to be an increasing and saturating function. We have the following result.

Theorem 3.1. *Consider the system (3.1) subject to initial conditions $a(0) = a_0 \geq 0$, $b(0) = b_0 \geq 0$ and $c(0) = c_0 \geq 0$. Then system (3.1) is a dynamical system on the biologically feasible region*

$$D = \left\{(a,b,c) \in \mathbb{R}^3_+ : a + b + c \leq \frac{\kappa}{\alpha_m}\right\}.$$

The invariance of $\mathbb{R}^3_+$ together with the existence and uniqueness of local solution of system (3.1) ensures a dynamical system. Assuming dormant cells do not die, we have the following result.

Proposition 3.1. *System (3.1) admits the following equilibria:*

(1) *a unique microbial-free state $E_0 = (0, 0, \beta g(0))$, and*
(2) *assuming $c^* - \beta g(0) \geq 0$, there exists zero or two coexistence states, or*
(3) *assuming $c^* - \beta g(0) < 0$, there exists a unique coexistence state.*

Proof. First, setting the right hand side of system (3.1) to zero, we obtain E_0 and $E^* = (a^*, b^*, c^*)$ where $a^* = \frac{rq(V^*)}{sp(U^*)}b^*$, with b^* and c^* satisfying $b^* - \alpha(\beta g(b^*) - c^*) = 0$ and $f(c^*) - 1 = 0$, respectively.

Next, defining $H_1(c^*) = f(c^*) - 1$, then $H_1(c^*)$ is a monotonically increasing function since $H_1'(c^*) = f'(c^*) \geq 0$, where we have used hypothesis $\mathcal{G}$. Furthermore, $\lim_{c^*\to 0^+} H_1(c^*) = -1 < 0$, therefore, a unique solution c^* satisfying $H_1(c^*) = f(c^*) - 1$ exists.

Finally, if we define $H_2(b^*) = b^* - \alpha(\beta g(b^*) - c^*) = 0$ with $c^* > 0$, then we notice that $\lim_{b^*\to+\infty} H_2(b^*) = +\infty$ and $\lim_{b^*\to 0^+} H_2(b^*) = \alpha(c^* - \beta g(0))$. In addition, $H_2'(b^*) = 1 - \alpha\beta g'(b^*)$ and $H_2''(b^*) = -\alpha\beta g''(b^*) \geq 0$ using the assumptions on $g(b)$. Hence $H_2'(b^*)$ is a monotonically increasing function with at most one root. If $c^* - \beta g(0) > 0$, then $H_2(b^*)$ has zero or two positive roots. If $c^* - \beta g(0) < 0$, then we have a unique positive root with $1 - \alpha\beta g'(b^*) > 0$. □

We notice that, unlike the work [27], here the third equilibrium on the boundary $b = 0$ does not exist since our model assumes $p(U) \neq 0$ for all U, see hypothesis $\mathcal{H}_2$. In particular, if $p(U) = 0$ then the initial state, $b = 0$, will not activate. See

for instance [10] for further details. To study the stability of equilibria, we consider the Jacobian matrix of system (3.1). At E_0, we have

$$J(E_0) = \begin{pmatrix} -sp(U_0) & rq(V_0) & 0 \\ sp(U_0) & f(\beta g(0)) - 1 - rq(V_0) & 0 \\ 0 & \alpha\beta g'(0) - f(\beta g(0)) & -\alpha \end{pmatrix}.$$

Clearly, $-\alpha$ is one of the eigenvalues of $J(E_0)$. Remaining eigenvalues come from the reduced matrix

$$\begin{pmatrix} -sp(U_0) & rq(V_0) \\ sp(U_0) & f(\beta g(0)) - 1 - rq(V_0) \end{pmatrix},$$

whose trace is $(f(\beta g(0)) - 1) - rq(V_0) - sp(U_0)$ and the determinant given by $-sp(U_0)(f(\beta g(0)) - 1)$. Under the hypotheses $\mathcal{H}_1$ and $\mathcal{H}_2$, with $U \geq 0$ and $V \geq 0$, we have the following result.

Proposition 3.2. *For any $U \in \{b, c\}$ and $V \in \{b, c\}$, the microbial-free equilibrium state E_0 is locally asymptotically stable provided $f(\beta g(0)) < 1$ and unstable if $f(\beta g(0)) > 1$.*

For later reference, it is important to note that Propositions 3.1 and 3.2, together with hypothesis $\mathcal{G}$ show that the condition $f(\beta g(0)) < 1$ is equivalent to $\beta g(0) < c^*$, and this refers to the population under starvation. This condition implies that the microbial population become extinct if the nutrient supply is less than some production threshold rate, $\beta g(0)$. Similarly, $f(\beta g(0)) > 1$ is equivalent to $\beta g(0) > c^*$, and the microbial life is sustained.

Next, we consider the local stability of the coexistence equilibrium under different combination of functions $p(U)$ and $q(V)$, i.e., study the dynamics of the model when the microbial activity is either random as a result of paracrine signalling or a direct consequence of the change in nutrient levels. We restrict our work to switch functions satisfying hypotheses $\mathcal{H}_1$ and $\mathcal{H}_2$. Neglecting dormant cell mortality, with switch from either hibernation or reawakening dependent on the nutrient levels, i.e., $q = q(c)$, and $p = p(c)$, the Jacobian matrix at the co-existence equilibrium is

$$J(E^*) = \begin{pmatrix} -sp(c^*) & rq(c^*) & rq'(c^*)b^* - sp'(c^*)a^* \\ sp(c^*) & -rq(c^*) & b^*f'(c^*) - rq'(c^*)b^* + sp'(c^*)a^* \\ 0 & \alpha\beta g'(b^*) - f(c^*) & -\alpha - b^*f'(c^*) \end{pmatrix},$$

where prime denotes differentiation with respect to the indicated variable. The characteristic equation of the Jacobian is given by

$$Q(\lambda) := \lambda^3 + s_1\lambda^2 + s_2\lambda + s_3 = 0,$$

with coefficients given by

$$\begin{aligned} s_1 &= -\text{trace}\, J(E^*) = sp(c^*) + rq(c^*) + b^*f'(c^*) + \alpha, \\ s_2 &= (sp(c^*) + rq(c^*))\big(\alpha + b^*f'(c^*)\big) + \big(1 - \alpha\beta g'(b^*)\big)\big(b^*f'(c^*) - rq'(c^*)b^* + sp'(c^*)a^*\big), \\ s_3 &= -\det J(E^*) = sp(c^*)b^*f'(c^*)\{1 - \alpha\beta g'(b^*)\}. \end{aligned}$$

Clearly, all coefficients are positive using hypothesis $\mathcal{G}$ provided $1 - \alpha\beta g'(b^*) > 0$. It remains to show that the second Hurwitz determinant Δ_2, is positive. We have

$$\begin{aligned} \Delta_2 &= s_1s_2 - s_3 \\ &= sp(c^*)b^*f'(c^*)\{\alpha\beta g'(b^*) - f(c^*)\} + \big[sp(c^*) + rq(c^*) + \big(\alpha + b^*f'(c^*)\big)\big] \\ &\quad \times\big[(sp(c^*) + rq(c^*))\big(\alpha + b^*f'(c^*)\big) - \big(\alpha\beta g'(b^*) - f(c^*)\big)\big(b^*f'(c^*) - rq'(c^*)b^* + sp'(c^*)a^*\big)\big] \\ &= (sp(c^*) + rq(c^*))\big(\alpha + b^*f'(c^*)\big)\big[sp(c^*) + rq(c^*) + \alpha + b^*f'(c^*)\big] \\ &\quad + \{1 - \alpha\beta g'(b^*)\}\big(b^*f'(c^*) - rq'(c^*)b^* + sp'(c^*)a^*\big)\big[rq(c^*) + \alpha + b^*f'(c^*)\big]. \end{aligned}$$

The trace as well as the second Hurwitz determinant are negative and positive, respectively. Therefore, the co-existence equilibrium is asymptotically stable, locally provided $1 - \alpha\beta g'(b^*) > 0$ with $f(\beta g(0)) > 1$. Similar arguments can be used for the local stability analysis of the other combinations of switch functions.

We summarise the results for the uniform steady state in Proposition 3.3 and Table 1 for different combinations of switch functions. In particular, the equilibria are either locally asymptotically stable (LAS) or may become unstable through Hopf bifurcation leading to oscillatory solutions (*boom-and-bust*).

Proposition 3.3. *Assume $1 - \alpha\beta g'(b^*) > 0$ and $\beta g(0) > c^*$:*

Case 1. *If $p = p(c)$ and $q = q(c)$, the co-existence equilibrium E^* is locally asymptotically stable.*
Case 2. *If $p = p(b)$ and $q = q(b)$, the co-existence equilibrium E^* is locally asymptotically stable provided $sp(b^*) + rq'(b^*)b^* \geq 0$.*
Case 3. *If $p = p(c)$ and $q = q(b)$, the co-existence equilibrium E^* is locally asymptotically stable.*
Case 4. *If $p = p(b)$ and $q = q(c)$, the co-existence equilibrium E^* is locally asymptotically stable.*

Remark 3.1. A comment on the condition $1 - \alpha\beta g'(b^*) < 0$ is necessary. We note that Propositions 3.1 and 3.2 together with hypothesis $\mathcal{G}$ show that the condition $f(\beta g(0)) < 1$ is equivalent to $\beta g(0) < c^*$. From the existence results

Table 1
Summary of Propositions 3.1, 3.2 and 3.3. The equilibrium points are locally asymptotically stable (LAS), unstable or we see sustained oscillatory solutions (*boom-and-bust*).

Equilibrium	Case	Sufficient condition	Necessary condition	Long term dynamics
E_0	$p(U)$, $q(V)$		$f(\beta g(0)) > 1$	Unstable
			$f(\beta g(0)) < 1$	LAS
E^*	$p(c)$, $q(c)$		$1 - \alpha\beta g'(b^*) > 0$	LAS
E^*	$p(b)$, $q(b)$	$sp(b^*) + rq'(b^*)b^* \geq 0$	$1 - \alpha\beta g'(b^*) > 0$	LAS
		$sp(b^*) + rq'(b^*)b^* < 0$	$1 - \alpha\beta g'(b^*) > 0$	*boom-and-bust*
E^*	$p(c)$, $q(b)$		$1 - \alpha\beta g'(b^*) > 0$	LAS
E^*	$p(b)$, $q(c)$		$1 - \alpha\beta g'(b^*) > 0$	LAS

in Proposition 3.1 and stability results summerised in Proposition 3.3 (and Table 1), the condition $1 - \alpha\beta g'(b^*) < 0$ and $f(\beta g(0)) < 1$ corresponds to an unstable coexistence equilibrium E^*. The bacteria-free state E_0 is locally asymptotically stable provided $f(\beta g(0)) < 1$ irrespective of the dependence in the switch functions. In particular, this describes the dynamics of the model under poor-nutrient conditions.

4. Traveling waves

From the simplest to the most complex biological levels of organisation, quiescent stages are found although different naming for each case may occur for diverse phenomena. For instance, mammals hibernate, genes become suppressed, tumour cells become dormant, and nerve cells rest. The previous section focused on the temporal nutrient-microbial interaction model with an assumption of homogeneous distribution. In practice, model (3.1) is not realistic, the space component is thereof very important since the active population bias-randomly move for the nutrient uptake to occur, which also result in proliferation, see for example [22,23]. Dispersal of active population, as well as that of the limiting nutrient must be considered.

In this section, we assume that dormant cell do not die and restrict ourselves to the case where switch of a state depends on the availability of limiting nutrient with $1 - \alpha\beta g'(b^*) > 0$ and $f(\beta g(0)) - 1 > 0$. Other forms can also be considered. We recall the one-dimensional sub-model of (2.3), which we restate as follows

$$\boldsymbol{u}_t = D\boldsymbol{u}_{xx} + G(\boldsymbol{u}), \quad x \in \mathbb{R},\ t > 0, \tag{4.1}$$

where

$$\boldsymbol{u} = (a, b, c)^t, \quad D = \operatorname{diag}(0, 1, d_c), \quad G(\boldsymbol{u}) = \begin{pmatrix} rq(c)b - sp(c)a \\ (f(c) - 1)b - rq(c)b + sp(c)a \\ \alpha(\beta g(b) - c) - bf(c) \end{pmatrix}. \tag{4.2}$$

For this system, the only equilibria are: $\mathbf{0} = (0, 0, \beta g(0))^T$ and $\mathbf{1} = (a^*, b^*, c^*)^T$. Now we have the following result.

A traveling-wave solution for system (2.3) is a nonnegative and bounded solution in the form of $\boldsymbol{u}(x, t) = (a(x, t), b(x, t), c(x, t))^T = (u(z), v(z), w(z))^T$, $z = x + \zeta t$, where $\zeta > 0$ is referred to as traveling-wave speed. We seek to find a traveling wave which can be viewed as a heteroclinic orbit connecting the two equilibria $\mathbf{1}$ and $\mathbf{0}$. It can be monotone or oscillatory. Substituting $\boldsymbol{u}(x, t) = (u(z), v(z), w(z))^T$ into (4.1) we obtain

$$\begin{cases} \zeta u' &= rq(w)v - sp(w)u, \\ \zeta v' &= v'' + (f(w) - 1)v - rq(w)v + sp(w)u, \\ \zeta w' &= d_c w'' + \alpha(\beta g(v) - w) - vf(w), \end{cases} \tag{4.3}$$

where prime denotes differentiation with respect to z. The asymptotic conditions for (4.3) are given as follows

$$\begin{cases} u(-\infty) &= a^*, \quad u(\infty) = 0, \\ v(-\infty) &= b^*, \quad v(\infty) = 0, \\ w(-\infty) &= c^*, \quad w(\infty) = \beta g(0). \end{cases} \tag{4.4}$$

First, we study the eigenvalue problem of the wave profile at the bacteria-free state $\mathbf{0} = (0, 0, \beta g(0))^T$. Linearising the equations at this point yields

$$\begin{cases} \zeta u' &= rq(\beta g(0))v - sp(\beta g(0))u, \\ \zeta v' &= v'' + v(f(\beta g(0)) - 1) - rq(\beta g(0))v + sp(\beta g(0))u, \\ \zeta w' &= d_c w'' + \alpha(v\beta g'(0) - w) - vf(\beta g(0)). \end{cases} \tag{4.5}$$

We further reduce the number of equations in (4.5) to two. Indeed, together with boundary conditions (4.4) we use the first equation of system (4.5) to express $u(z)$ in terms of $v(z)$, i.e.,

$$u(z) = \frac{rq(\beta g(0))}{\zeta} \int_{-\infty}^{z} v(\xi) e^{\frac{sp(\beta g(0))}{\zeta}(z-\xi)} d\xi. \tag{4.6}$$

Substituting (4.6) into (4.5) leads to

$$\begin{aligned}\zeta v' &= v'' + v(f(\beta g(0)) - 1) - rq(\beta g(0))v + sp(\beta g(0))\tfrac{rq(\beta g(0))}{\zeta}\int_{-\infty}^{z} v(\xi)e^{\frac{sp(\beta g(0))}{\zeta}(z-\xi)}d\xi,\\ \zeta w' &= d_c w'' + \alpha(v\beta g'(0) - w) - vf(\beta g(0)).\end{aligned} \tag{4.7}$$

By substituting $v(z) = e^{\lambda z}$ into the first equation of system (4.7), we have the characteristic equation

$$\lambda^2 - \zeta\lambda + (f(\beta g(0)) - 1) - rq(\beta g(0)) + \frac{sp(\beta g(0))rq(\beta g(0))}{\zeta(\lambda + sp(\beta g(0))/\zeta)} = 0,$$

or

$$P(\lambda) := \lambda^3 + a_2\lambda^2 + a_1\lambda + a_0 = 0, \tag{4.8}$$

with

$$\begin{aligned}a_2 &= \frac{sp(\beta g(0))}{\zeta} - \zeta,\\ a_1 &= (f(\beta g(0)) - 1) - sp(\beta g(0)) - rq(\beta g(0)),\\ a_0 &= \frac{sp(\beta g(0))}{\zeta}(f(\beta g(0)) - 1).\end{aligned}$$

Now, we have two cases depending on the sign of a_1: $f(\beta g(0)) - 1 < sp(\beta g(0)) + rq(\beta g(0))$ or $f(\beta g(0)) - 1 \geq sp(\beta g(0)) + rq(\beta g(0))$. As we will see later in the discussion of Lemma 4.1, the case $f(\beta g(0)) - 1 > sp(\beta g(0)) + rq(\beta g(0))$ does not guarantee the existence of $\zeta^* > 0$ where ζ^* is the minimal wave speed, and will not be considered further.

Lemma 4.1. *Assume $f(\beta g(0)) - 1 > 0$. Then there exists $\zeta^* > 0$ and $\lambda^* > 0$ such that*

$$P(\lambda^*) = 0, \quad \text{and} \quad \left.\frac{\partial P}{\partial\lambda}\right|_{\lambda=\lambda^*} = 0. \tag{4.9}$$

The result in Lemma 4.1 is similar to the discussion in [30]. For completeness, we will provide the outline of the proof here. Since $f(\beta g(0)) - 1 > 0$, we see that (4.9) has one negative root and two roots with positive real parts. By calculation, to identify the conditions under which these two roots are positive real numbers, we have

$$\begin{aligned}P(\zeta) &= \frac{sp(\beta g(0))}{\zeta}(f(\beta g(0)) - 1) > 0,\\ P_1(\lambda) := \frac{1}{3}\frac{\partial P}{\partial\lambda} &= \lambda^2 + \frac{2}{3}\left(\frac{sp(\beta g(0))}{\zeta} - \zeta\right)\lambda + \frac{1}{3}((f(\beta g(0)) - 1) - sp(\beta g(0)) - rq(\beta g(0))).\end{aligned}$$

We see that $P_1(\lambda)$ has a unique positive root

$$\lambda^* = \frac{1}{3}\frac{\zeta^2 - sp(\beta g(0)) + \sqrt{\zeta^4 + sp(\beta g(0))[\zeta^2 + sp(\beta g(0))] - 3\zeta^2[(f(\beta g(0)) - 1) - rq(\beta g(0))]}}{\zeta},$$

provided $f(\beta g(0)) - 1 \leq rq(\beta g(0))$. Since $P(\zeta)$ is positive, then equation (4.8) has two positive roots if and only if $P(\lambda^*) < 0$, otherwise, there exists two complex roots with positive real parts if $P(\lambda^*) > 0$.

To obtain the minimal wave speed, we transform (4.8) to get an expression giving its discriminant, i.e., an expression in terms of the parameters. Suppose

$$\begin{aligned}P(\lambda) &= P_1(\lambda)Q_1(\lambda) + R_1(\lambda),\\ P_1(\lambda) &= R_1(\lambda)Q_2(\lambda) + R_2(\zeta, \beta),\end{aligned}$$

where $Q_1(\lambda)$, $R_1(\lambda)$ are the quotient and remainder terms when $P(\lambda)$ is divided by $P_1(\lambda)$, respectively. Similarly, $Q_2(\lambda)$, $R_2(\zeta, \beta g(0))$ are the quotient and remainder terms of $P_1(\lambda)$ divided by $R_1(\lambda)$. Obviously, when $R_2(\zeta, \beta g(0)) = 0$, then $P(\lambda^*) = P_1(\lambda^*) = 0$. The sign of $-R_2(\zeta, \beta g(0))$ is determined by

$$\Delta(\zeta, \beta g(0)) = b_0\zeta^6 + b_1\zeta^4 + b_2\zeta^2 + b_3, \tag{4.10}$$

where $\Delta(\zeta, \beta g(0))$ is the discriminant of Eq. (4.8) and

$$\begin{aligned}b_0 &= s^2p(\beta g(0))^2 + 2sp(\beta g(0))(f(\beta g(0)) - 1 + rq(\beta g(0))) + (rq(\beta g(0)) - (f(\beta g(0)) - 1))^2,\\ b_1 &= 2s^3p(\beta g(0))^3 + 2s^2p(\beta g(0))^2(4rq(\beta g(0)) - (f(\beta g(0)) - 1))\\ &\quad + 2sp(\beta g(0))(5rq(\beta g(0)) + 4(f(\beta g(0)) - 1)(rq(\beta g(0)) - (f(\beta g(0)) - 1)))\\ &\quad + 4(rq(\beta g(0)) - (f(\beta g(0)) - 1))^3,\\ b_2 &= s^4p(\beta g(0))^4 + 2s^3p(\beta g(0))^3(rq(\beta g(0)) - 4(f(\beta g(0)) - 1))\\ &\quad + s^2p(\beta g(0))^2(r^2q(\beta g(0))^2 - 20rq(\beta g(0))(f(\beta g(0)) - 1) - 8(f(\beta g(0)) - 1)^2),\end{aligned}$$

$$b_3 = -4s^4 p(\beta g(0))^4 (f(\beta g(0)) - 1).$$

From Eq. (4.10), we notice that $b_0 > 0$, $b_1 > 0$ provided $f(\beta g(0)) - 1 \le rq(\beta g(0))$ and $b_3 < 0$ since $f(\beta g(0)) - 1 > 0$. Using Descarte's rule of signs, it follows that there is a unique $\zeta^* > 0$ such that $\Delta(\zeta^*, \beta g(0)) = 0$, and this implies

$$\Delta(\zeta, \beta g(0)) \begin{cases} < 0 & \text{if } \zeta \in (0, \zeta^*), \\ = 0 & \text{if } \zeta = \zeta^*, \\ > 0 & \text{if } \zeta > \zeta^*. \end{cases}$$

Direct calculations show that $P(\lambda^*) = P_1(\lambda^*) = 0$ is valid when $\zeta = \zeta^*$ and $P(\lambda)$ is a decreasing function of ζ. Hence, we conclude that for $\zeta > \zeta^*$, $P(\lambda^*) < 0$ (we have two positive roots), for $\zeta \in (0, \zeta^*)$, $P(\lambda^*) > 0$, (we have two complex roots), and we have only one positive root if $\zeta = \zeta^*$. We now state the following result.

Theorem 4.1. *Assume $f(\beta g(0)) - 1 \le rq(\beta g(0))$ and $f(\beta g(0)) - 1 > 0$. There exists a minimal wave speed $\zeta^* > 0$, which is a unique positive root of (4.10). When $\zeta \ge \zeta^*$, the system has a traveling wave solution satisfying boundary conditions (4.4). When $0 < \zeta < \zeta^*$, system (3.1) has no traveling wave solution satisfying conditions (4.4).*

The complete proof of Theorem 4.1 will not be considered here. Interested readers can consult, for example, [30] and references therein. By the method of linearization, we have shown that system (4.3) admits the minimal wave speed, ζ^*, which is the unique root of (4.10). Thus, it remains to show the existence of traveling wave solution for system (4.3), see Remark 4.1.

Remark 4.1. In [31], the authors applied the methods of Wazewski Theorem, LaSalle's Invariance Principle and Hopf bifurcation theory to prove the existence of traveling waves which is hard to apply for three state variable system (4.1). Moreover, we cannot employ the approach used in monotone wavefronts for cooperative systems [32] since our system (4.1) is not cooperative, that is, has similar interactions as predator-prey models. In [25], the authors considered constant conversion rates to show existence of traveling waves on an auxiliary system for a bacterial colony model with transitions between active and inactive bacteria. From the auxiliary system, they constructed upper and lower solutions for their original system of equations. Therefore, the technique of constructing a pair of upper and lower solutions and the application of *Schauder* Fixed point method is relevant here to show the existence of traveling waves for system (4.1) using the same arguments as in [25,30].

5. Numerical results

Since the pioneering monograph by Mickens on the subject [33], the nonstandard finite difference method has been applied successfully to solve several differential models in the applied sciences, see [34] for a latest review. In this section, we propose a nonstandard-finite difference scheme to solve the proposed reaction-diffusion system. First we recall the differential model (3.1). We let $(a^n, b^n, c^n)^T$ denote an approximation of $(a(t_n), b(t_n), c(t_n))^T$ where $t_n = nk$, with $n = 1,2,3,\ldots$ and $k = \Delta t > 0$. We propose the following scheme constructed via non-local approximation (cf [33].) of nonlinear terms

$$\begin{cases} \dfrac{a^{n+1} - a^n}{\phi(k)} = rq(V^n)b^n - sp(U^n)a^{n+1} - a^{n+1}, \\ \dfrac{b^{n+1} - b^n}{\phi(k)} = c^n h(c^n)b^n - b^{n+1} - rq(V^n)b^{n+1} + sp(U^n)a^{n+1}, \\ \dfrac{c^{n+1} - c^n}{\phi(k)} = \alpha(\beta g(b^n) - c^{n+1}) - c^{n+1}h(c^n)b^{n+1}, \end{cases} \tag{5.1}$$

where the denominator function of discrete derivatives is chosen according to (3.2) with $\phi(k) = k + \mathcal{O}(k^2)$. In particular, we see that (3.2) has an exact scheme (see [33])

$$\frac{\omega^{n+1} - \omega^n}{\phi(k)} \le \frac{\kappa}{\alpha_m} - \omega^{n+1}, \tag{5.2}$$

with $\phi(k) = \exp(\alpha_m k) - 1$. By exact scheme, we mean that the discrete solution w^n coincides with the continuous solution $w(t_n)$. In compact form, we rewrite system (5.1) to get

$$\boldsymbol{u}^{n+1} = F(k)(\boldsymbol{u}^n), \quad \boldsymbol{u}(0) = \boldsymbol{u}_0,$$

where $\boldsymbol{u}^n = (a^n, b^n, c^n)$, and

$$F(k)(\boldsymbol{u}^n) = \begin{pmatrix} \dfrac{a^n + \phi rq(V^n)b^n}{1 + \phi + \phi sp(U^n)} \\ \dfrac{b^n + \phi c^n h(c^n)b^n + \phi sp(U^n)a^{n+1}}{1 + \phi + \phi rq(V^n)} \\ \dfrac{c^n + \phi\alpha\beta g(b^n)}{1 + \alpha\phi + \phi h(c^n)b^{n+1}} \end{pmatrix}, \tag{5.3}$$

where

$$a^{n+1}=\frac{a^n+\phi rq(V^n)b^n}{1+\phi+\phi sp(U^n)},\quad \text{and}\quad b^{n+1}=\frac{b^n+\phi c^n h(c^n)b^n+\phi sp(U^n)a^{n+1}}{1+\phi+\phi rq(V^n)}.$$

Using standard techniques [33,35], we now verify dynamic consistency of the scheme. For consistency, F must satisfy the following requirements

$$F(0)(\boldsymbol{u})=\boldsymbol{u},\quad \frac{dF(0)}{dk}(\boldsymbol{u})=F(\boldsymbol{u}).$$

Clearly, the first condition is satisfied. We also have that $\frac{dF(0)}{dk}(\boldsymbol{u})\Big|_{k=0}$ is given by

$$\begin{pmatrix}\frac{rq(V)b-sp(U)a-a}{(1+\phi+\phi sp(U))^2}\\ \frac{(ch(c)-1)b-rq(V)b+sp(U)a}{(1+\phi+\phi rq(V))^2}\\ \frac{\alpha(\beta g(b)-c)-bch(c)}{(1+\alpha\phi+\phi h(c)b)^2}\end{pmatrix}_{k=0}=\begin{pmatrix}rq(V)b-sp(U)a-a\\ (ch(c)-1)b-rq(V)b+sp(U)a\\ \alpha(\beta g(b)-c)-bch(c)\end{pmatrix}=F(\boldsymbol{u})$$

Hence the nonstandard finite difference scheme (5.1) is consistent with the differential model (3.1). The above discrete system (5.3) can be rewritten in the explicit form

$$A(k,\boldsymbol{u}^n)\boldsymbol{u}^{n+1}=B(k,\boldsymbol{u}^n)\boldsymbol{u}^n+(0,0,\alpha\beta g(b^n))^T, \tag{5.4}$$

where matrices $A(k,\boldsymbol{u}^n)$ and $B(k,\boldsymbol{u}^n)$ are given by

$$\begin{pmatrix}1+\phi+\phi sp(U^n) & 0 & 0\\ 0 & (1+\phi+\phi rq(V^n))(1+\phi+\phi sp(U^n)) & 0\\ 0 & 0 & A_{33}\end{pmatrix},$$

where $A_{33}=1+\alpha\phi+\phi h(c^n)\left[\frac{b^n(1+\phi c^n h(c^n))(1+\phi+\phi sp(U^n))+\phi sp(U^n)(a^n+\phi rq(V^n)b^n)}{(1+\phi+\phi rq(V^n))(1+\phi+\phi sp(U^n))}\right]$ and

$$\begin{pmatrix}1 & \phi rq(V^n) & 0\\ \phi sp(U^n) & (1+\phi+\phi sp(U^n))(1+\phi c^n h(c^n))+\phi rq(V^n)\phi sp(U^n) & 0\\ 0 & \alpha\beta g'(b^n) & 1\end{pmatrix},$$

respectively. We see that $A(k,\boldsymbol{u}^n)$ is an *M-matrix* since it is a diagonal matrix. Hence, its inverse, $A(k,\boldsymbol{u}^n)^{-1}$, is non-negative. We have that $B(k,\boldsymbol{u}^n)\geq 0$, which is sufficient for the scheme to preserve the positivity of solutions. We conclude that scheme (5.1) defines a discrete dynamical system on the same domain as the continuous model (3.1). See for example [36] and references therein for more details. Setting $\boldsymbol{u}^{n+1}=\boldsymbol{u}^n$, we see that scheme (5.1) preserves the same fixed points, $E_0=(0,0,\beta g(0))$ and $E^*=(a^*,b^*,c^*)$ as the continuous model (3.1).

We now need to verify the preservation of the stability of fixed point. Following (5.3) and (5.4), and assuming the conversion rates are functions of c, that is, $p=p(c)$ and $q=q(c)$, then $F(k)(\boldsymbol{u})=A^{-1}(k,\boldsymbol{u})B(k,\boldsymbol{u})$ so that

$$\frac{dF(k)}{dy}(\boldsymbol{u})=\begin{pmatrix}\frac{1}{1+\phi+\phi sp(c)} & \frac{\phi rq(c)}{1+\phi+\phi sp(c)} & J_{1,3}\\ \frac{\phi sp(c)}{1+\phi+\phi rq(c)} & \frac{1+\phi ch(c)}{1+\phi+\phi rq(c)} & J_{2,3}\\ 0 & \frac{\phi\alpha\beta g'(b)}{1+\alpha\phi+\phi bh(c)}-\frac{(c+\phi\alpha\beta g(b))\phi h(c)}{(1+\alpha\phi+\phi bh(c))^2} & J_{3,3}\end{pmatrix},$$

where

$$J_{1,3}=\frac{\phi rq'(c)}{1+\phi+\phi sp(c)}-\frac{(a+\phi rq(c)b)\phi sp'(c)}{(1+\phi+\phi sp(c))^2},$$

$$J_{2,3}=\frac{\phi\big(bh(c)+ch'(c)b\big)+\phi sp'(c)a}{1+\phi+\phi rq(c)}-\frac{\phi rq'(c)(b+\phi ch(c)b+\phi sp(c)a)}{(1+\phi+\phi rq(c))^2},$$

$$J_{3,3}=\frac{1}{1+\alpha\phi+\phi bh(c)}-\frac{\phi h'(c)b(c+\phi\alpha\beta g(b))}{(1+\alpha\phi+\phi bh(c))^2}.$$

We proceed to show that all eigenvalues of the Jacobian evaluated at the fixed points lie in a unit circle.

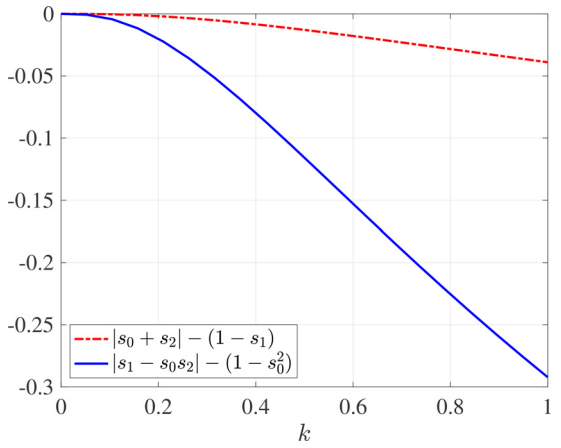

Fig. 1. Numerical illustration for the local stability of the co-existence fixed point E^*.

Evaluating $\frac{dF(k)}{d\boldsymbol{u}}(\boldsymbol{u})$ at the bacteria-free equilibrium, we obtain

$$\frac{dF(k)}{d\boldsymbol{u}}(0,0,\beta g(0)) = \begin{pmatrix} \frac{1}{1+\phi+\phi sp(\beta g(0))} & \frac{\phi rq(\beta g(0))}{1+\phi+\phi sp(\beta g(0))} & 0 \\ \frac{\phi sp(\beta g(0))}{1+\phi+\phi rq(\beta g(0))} & \frac{1+\phi\beta g(0)h(\beta g(0))}{1+\phi+\phi rq(\beta g(0))} & 0 \\ 0 & \frac{\phi\alpha\beta g'(0)}{1+\alpha\phi} - \frac{(\beta g(0)+\phi\alpha\beta g(0))\phi h(\beta g(0))}{(1+\alpha\phi)^2} & \frac{1}{1+\alpha\phi} \end{pmatrix}.$$

Now, we need to verify that all eigenvalues of the Jacobian matrix at E_0 lie inside a unit circle. First, we see that $\frac{1}{1+\alpha\phi}$ is the first eigenvalue of the matrix $\frac{dF(k)}{d\boldsymbol{u}}(0,0,\beta g(0))$ which is strictly less than one. The remaining eigenvalues are found from the reduced matrix

$$J_r = \begin{pmatrix} \frac{1}{1+\phi+\phi sp(\beta g(0))} & \frac{\phi rq(\beta g(0))}{1+\phi+\phi sp(\beta g(0))} \\ \frac{\phi sp(\beta g(0))}{1+\phi+\phi rq(\beta g(0))} & \frac{1+\phi\beta g(0)h(\beta g(0))}{1+\phi+\phi rq(\beta g(0))} \end{pmatrix}.$$

To prove that all the remaining eigenvalues lie in a unit circle, we use the well-known Jury?s conditions for $J_r \in \mathbb{R}^2 \times \mathbb{R}^2$. In this case, we need to show that

$$(i)\quad 1-\det(J_r) > 0, \quad (ii)\quad 1-\text{trace}(J_r)+\det(J_r) > 0, \quad (iii)\quad 0 < J_{11} < 1,\ 0 < J_{22} < 1.$$

The first condition, $1-\det(J_r) > 0$, is equivalent to

$$\phi[2\phi sp(\beta g(0))rq(\beta g(0)) + (\phi+1)(sp(\beta g(0)) + rq(\beta g(0)) + 1) + (1-\beta g(0)h(\beta g(0)))] > 0,$$

which is strictly positive provided $\beta g(0)h(\beta g(0)) < 1$ or $f(\beta g(0)) < 1$. The second condition is equivalent to

$$\phi^2[(1-\beta g(0)h(\beta g(0)))(1+sp(\beta g(0))) + rq(\beta g(0))],$$

which is strictly positive provided $f(\beta g(0)) = \beta g(0)h(\beta g(0)) < 1$. The last condition is clearly satisfied provided $\beta g(0)h(\beta g(0)) < 1$, hence the fixed point E_0 is locally asymptotically stable provided $f(\beta g(0)) < 1$, and unstable if $f(\beta g(0)) > 1$.

Similarly, for the stability of E^*, we proceed to evaluate $\frac{dF(k)}{d\boldsymbol{u}}(\boldsymbol{u})$ at the co-existence fixed point and we obtain the characteristic equation

$$\lambda^3 + s_2\lambda^2 + s_1\lambda + s_0 = 0, \tag{5.5}$$

where the roots of Eq. (5.5) lie inside the unit circle provided

$$|s_0+s_2| < 1+s_1, \quad \text{and} \quad |s_1-s_0s_2| < 1-s_0^2. \tag{5.6}$$

A theoretical verification of these conditions result to an overlong expression, thus we proceed numerically. In the results shown in Fig. 1, we choose $\alpha = 0.5$ and $\beta = 1.1$ with $1-\alpha\beta g'(b^*) > 0$. Clearly, for $k > 0$, conditions (5.6) are satisfied and

we conclude that all eigenvalues lie in a unit circle. Hence, the coexistence fixed point for the discrete model (5.1) is locally asymptotically stable provided $1-\alpha\beta g'(b^*)>0$.

Following the scheme (5.1), we apply the central difference approximation for second derivatives and propose the following scheme for one dimensional submodel of (2.3)

$$\begin{aligned}
\frac{a_m^{n+1}-a_m^n}{\phi(\Delta t)} &= rq(V_m^n)b_m^n - sp(U_m^n)a_m^{n+1} - a_m^{n+1},\\
\frac{b_m^{n+1}-b_m^n}{\phi(\Delta t)} &= \tfrac{1}{\psi(\Delta x)^2}\left[b_{m-1}^n - 2b_m^n + b_{m+1}^n\right] + c_m^n h(c_m^n)b_m^n - b_m^{n+1} - rq(V_m^n)b_m^{n+1} + sp(U_m^n)a_m^{n+1},\\
\frac{c_m^{n+1}-c_m^n}{\phi(\Delta t)} &= \tfrac{d_c}{\psi(\Delta x)^2}\left[c_{m-1}^n - 2c_m^n + c_{m+1}^n\right] + \alpha\left(\beta g(b_m^n) - c_m^{n+1}\right) - c_m^{n+1}h(c_m^n)b_m^{n+1},
\end{aligned} \tag{5.7}$$

where the numerical approximation of the unknown $\boldsymbol{u}(x,t)$ on a uniform grid is written as $\boldsymbol{u}_m^n$ at time $t^n = n\Delta t$ and spatial point $x_m = m\Delta x$ with $m = 0, 1, 2, \ldots, M$ and $n = 0, 1, 2, \ldots$. The function $\psi(\Delta x)$ satisfies the asymptotic relationship $\psi(\Delta x) = \Delta x + \mathcal{O}([\Delta x]^2)$. In explicit form, we write

$$\begin{cases}
a_m^{n+1} = \dfrac{a_m^n + \phi rq(V_m^n)b_m^n}{1+\phi+\phi sp(U_m^n)},\\[2ex]
b_m^{n+1} = \dfrac{\vartheta\,(b_{m-1}^n + b_{m+1}^n) + (1-2\vartheta)b^n + \phi c_m^n h(c_m^n)b_m^n + \phi sp(U_m^n)a_m^{n+1}}{1+\phi+\phi rq(V_m^n)},\\[2ex]
c_m^{n+1} = \dfrac{d_c\vartheta\,(c_{m-1}^n + c_{m+1}^n) + (1-2d_c\vartheta)c_m^n + \phi\alpha\beta g(b_m^n)}{1+\alpha\phi+\phi h(c_m^n)b_m^{n+1}}.
\end{cases} \tag{5.8}$$

The discretisation result in an explicit scheme with very low computational cost. The optimal time step and spatial step size are chosen according to the restriction specified for parabolic equations, i.e., $\vartheta = \dfrac{\phi}{\psi^2} \le \dfrac{1}{2}$ with $d_c \le 1$. The stability restriction also ensures for the preservation of positivity of solutions for scheme (5.8) in the sense that if $\boldsymbol{u}_m^n > 0$, then $\boldsymbol{u}_m^{n+1} > 0$.

5.1. Uniform steady state simulations

The transition functions are well documented in the literature. For example, the work [10] discussed to a greater extent the functions $p(u)$ and $q(v)$. The authors considered the transition between active and quiescent state by awakening and hibernation functions p and q, respectively, each being $\in (0,1)$ which can be thought of as probabilities of the population to switch states. We extend this discussion here to study the dynamics of model (3.1) under various combinations of variables u and v satisfying $\mathcal{H}_1$ and $\mathcal{H}_2$. In particular, the asymptotic behaviour when the transition is either a response to the rate-limiting nutrient concentration level or a result of paracrine signalling. Throughout, we assume that $f(c) = c$ (i.e., $h(c) = 1$) satisfying hypothesis $\mathcal{G}$, and

$$g(b) = \varepsilon + \frac{b^\kappa}{b_0^\kappa + b^\kappa}, \tag{5.9}$$

where b_0 is the half-saturation constant and we take $\kappa = 1$. As summarised in Table 1, it is the choice of switch functions and the switching rates that determine the dynamics of the model, in particular, Case 2. Following [10], hibernation and arousal functions take the form

$$q(V) = \frac{1}{1+V^\ell}, \qquad p(U) = \frac{\delta + U^\ell}{1+U^\ell}, \tag{5.10}$$

respectively, where ℓ is a positive integer. The modified arousal function is important since no activation is possible using the simple Hill function $U^\ell/(1+U^\ell)$. In this context, δ defines the minimum concentration/density at which the switch can take place.

In the numerical illustrations given in Figs. 2-5, we provide simulations for $\delta = 1.1$. For simulations not shown here, we highlight that smaller values of δ amplifies the oscillatory behaviour which disappears for larger values, see Figs. 3 and 4. In fact, in the limit $\delta \to 0$, the state $b = 0$ will not be activated. The rest of the parameters, unless stated differently in the figure caption, are given as follows: $r = s = \varepsilon = 1$ and $\ell = 5$ (for the Hill functions in (5.10)). Under poor-nutrient conditions or unfavourable conditions for proliferation, $\beta g(0) < c^* = 1$, the microbial population goes extinct irrespective of the dependence in the switch functions. That is, all trajectories will converge to the microbial-free equilibrium, see Figs. 2-5.

Remark 5.1. From here forthwith, we assume $1-\alpha\beta g'(b^*) > 0$ and $f(\beta g(0)) - 1 > 0$. The first condition, $1-\alpha\beta g'(b^*) > 0$, is necessary and of interest since it corresponds to the existence, uniqueness and local stability of E^*. Biologically, this condition implies that the biomass is sustained if the nutrient supply remains above a certain threshold value, $\beta g(0)$.

Remark 5.2. In boom-and-bust cases, hibernation is a result of cell-to-cell interaction, other than the availability of nutrient. Thus, the dependence of switch functions on cell-to-cell interaction is of importance in explaining the occurrence of self-sustained oscillations in microbial populations, see Fig. 3.

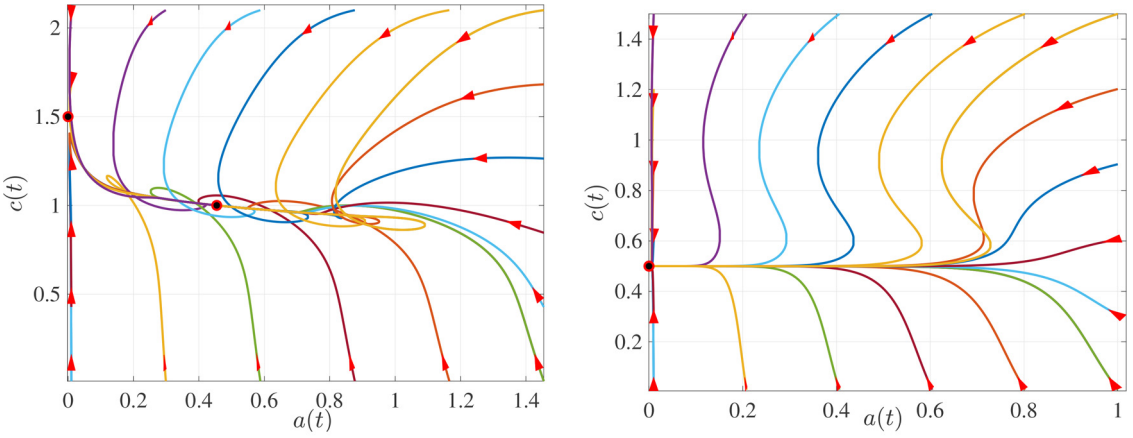

(a) Phase plane for $\beta g(0) > c^*$. (b) Phase plane for $\beta g(0) < c^*$.

Fig. 2. Case 1: In this case $p = p(c)$, $q = q(c)$ with $\alpha = 0.5$. In (a), $\beta = 1.1$ and all trajectories converge to the coexistence equilibrium point and in (b) $\beta = 0.5$ and all trajectories converge to the microbial-free equilibrium.

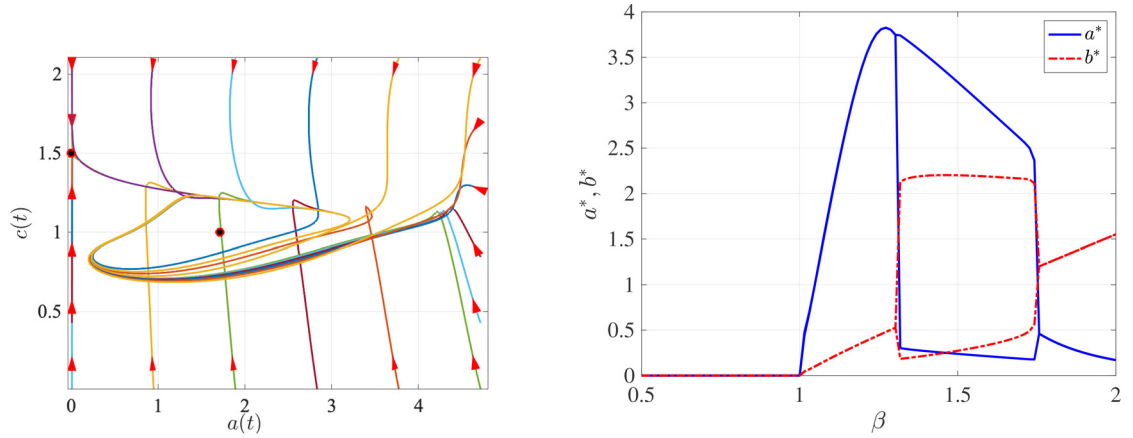

(a) Phase plane with $\beta g(0) > c^*$. (b) Bifurcation with respect to β.

Fig. 3. Case 2: In this case $p = p(b)$, $q = q(b)$ with $\alpha = 0.7$. The bifurcation figure shows transition from stable state through Hopf bifurcation leading to oscillatory solutions. Figure (b) shows the minimal and maximal values of dormant (solid line) and active biomass (broken line).

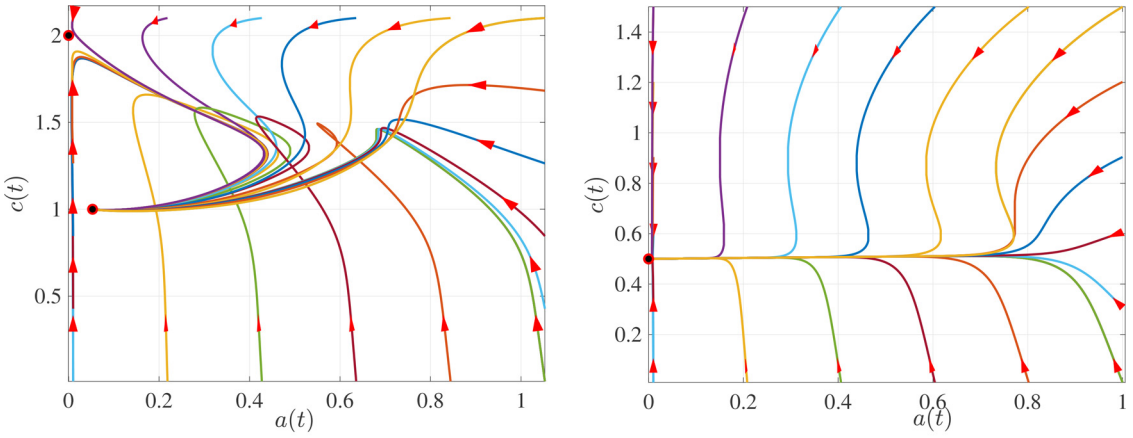

(a) Phase plane for $\beta g(0) > c^*$. (b) Phase plane for $\beta g(0) < c^*$.

Fig. 4. Case 3: In this case $p = p(c)$, $q = q(b)$ with $\alpha = 1.0$. In (a), $\beta = 2.0$ and all trajectories converge to the coexistence equilibrium point and in (b) $\beta = 0.5$ and all trajectories converge to the microbial-free equilibrium.

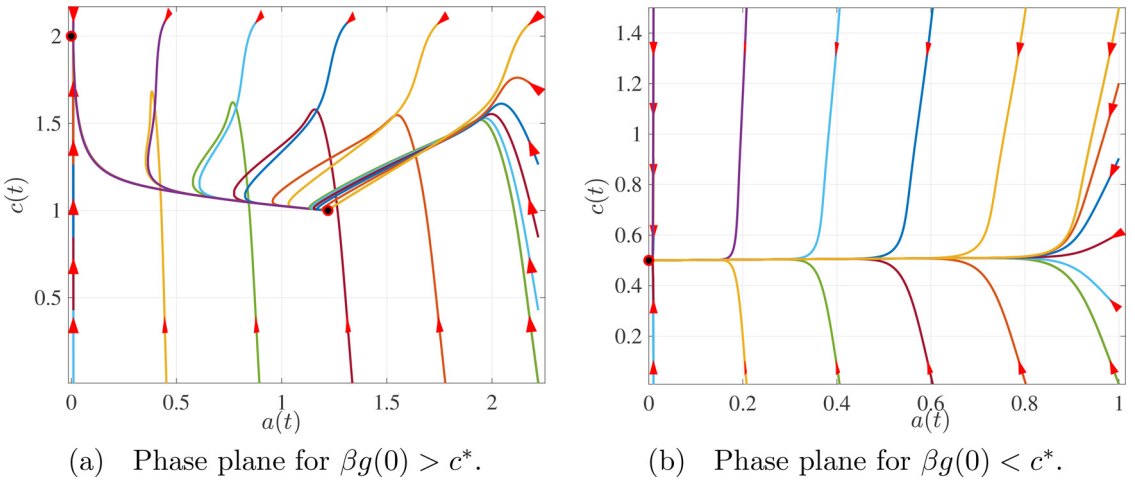

Fig. 5. Case 4: In this case $p = p(b)$, $q = q(c)$ with $\alpha = 1.0$. In (a), $\beta = 2.0$ and all trajectories converge to the coexistence equilibrium point and in (b) $\beta = 0.5$ and all trajectories converge to the microbial-free equilibrium.

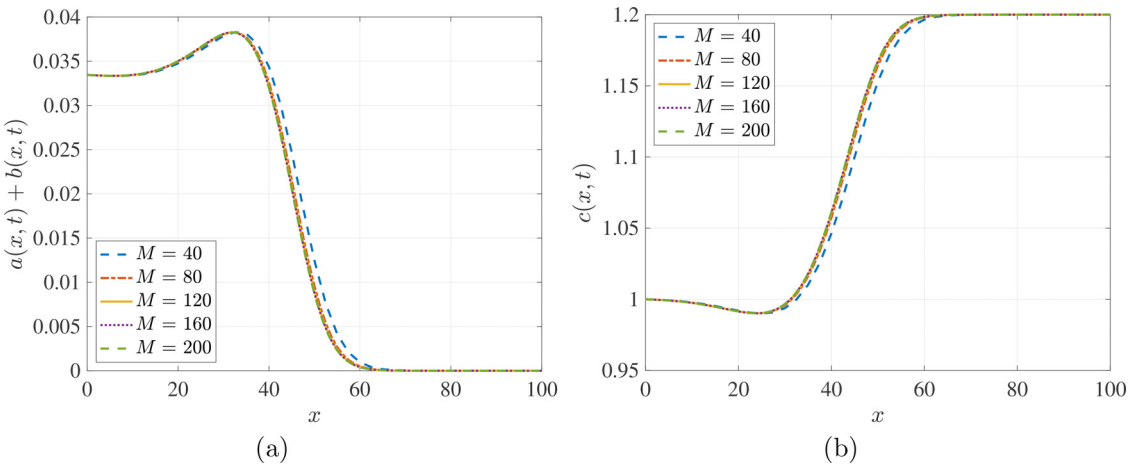

Fig. 6. Convergence results for $\beta = 1.2$ and $\alpha = 0.1$.

Remark 5.3. It is worth making a remark regarding the model formulation vis-á-vis the existence of plankton blooms (oscillatory solution). If we neglect the dormant state, then we have a simple model

$$\begin{cases} \dfrac{db}{dt} = (f(c) - 1)b, \\ \dfrac{dc}{dt} = \alpha(\beta g(b) - c) - bf(c), \end{cases} \tag{5.11}$$

with two nonzero equilibrium as before. The local stability of both equilibria remains the same, with E^* locally asymptotically stable provided $f(\beta g(0)) > 1$. This result, including Proposition 3.3, is consistent with the findings in [10]. Particularly, this formulation is not capable of explaining the observed oscillatory behavior in plankton populations.

5.2. Traveling wave simulations

In this section, we present numerical simulations to illustrate the above theoretical results for the reaction-diffusion model. We will further discuss the effects of threshold value β, and the switch rates r and s on the traveling wave speed. We perform one-dimensional numerical simulations for model (2.3) using scheme (5.8). In the interest of travelling wave solutions, the spatial domain is the truncated region $\Omega = (0, 100)$ with Dirichlet boundary conditions on $\partial\Omega$ specified as follows

$$\boldsymbol{u}(0, t) = (a^*, b^*, c^*) \quad \text{and} \quad \boldsymbol{u}(100, t) = (0, 0, \beta g(0)).$$

In Fig. 6 we present the convergence results for the proposed scheme. With $M = 120$, we observe that the solution profile is not affected by changes in step size, hence we use this number of grid points for the rest of the simulations presented in this paper.

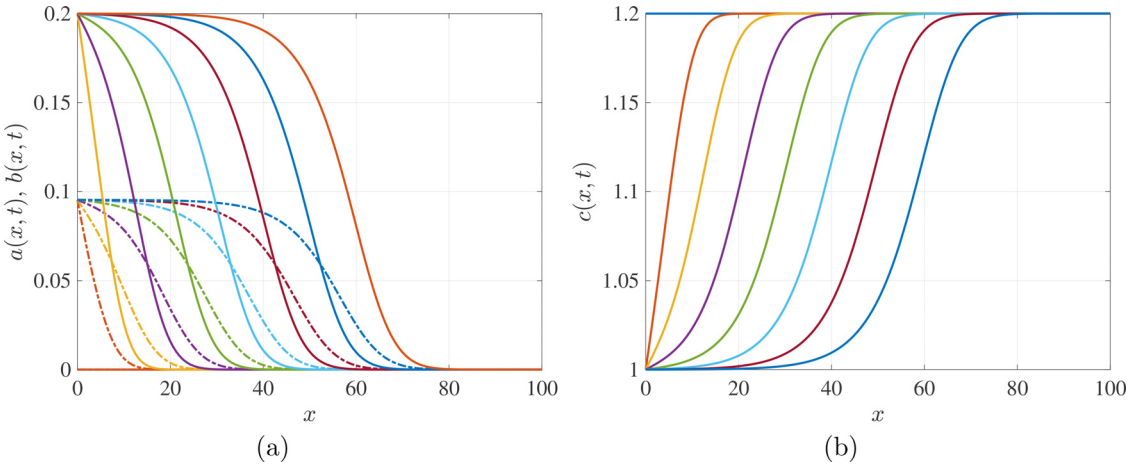

Fig. 7. Solution profiles at equally spaced intervals of 15 time units for $\beta = 1.2$ and $\alpha = 0.5$. In (a), the solid line denotes density b and the broken line denotes density a.

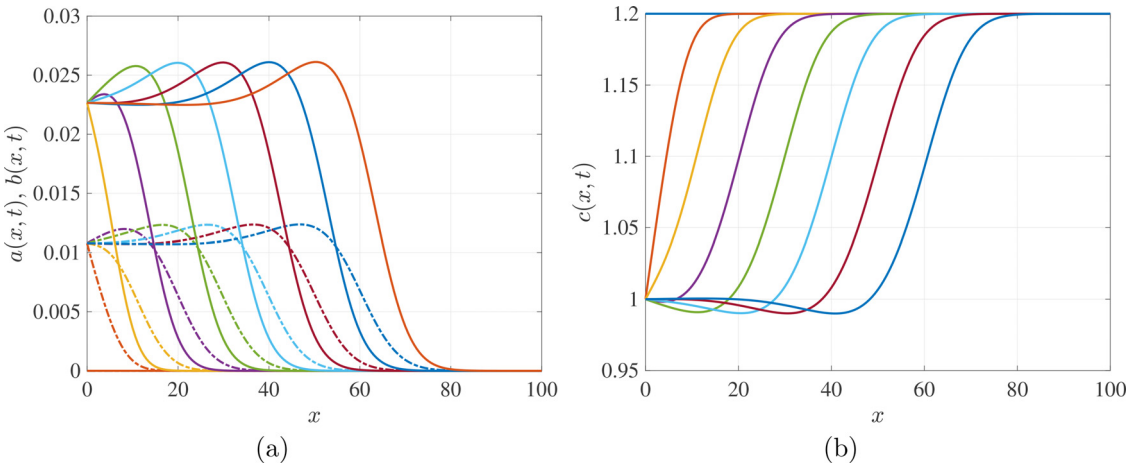

Fig. 8. Solution profiles at equally spaced intervals of 15 time units for $\beta = 1.2$ and $\alpha = 0.1$. In (a), the solid line denotes density b and the broken line denotes density a.

For the model under investigation, we wish to describe the spreading rate (traveling wave speed) of the plankton population from an initially bacteria population-free state. These results could formulate the possible propagation modes of biofilms and plankton populations. To illustrate our results, all simulations are performed with all parameters selected as before. Unless stated differently under figure captions, we also choose $d_c = 1$.

In Figs. 7 – 9, we present simulations to illustrate the existence of traveling waves for the reaction-diffusion system (4.1) with (4.2) using different values of α and β as stated under the figure captions. All parameters are fixed as stated before unless indicated otherwise. We observe wave solutions connecting the two equilibria: $\mathbf{1} = (a^*, b^*, c^*)$ and $\mathbf{0} = (0, 0, \beta g(0))$. In Fig. 7, we see that for $\beta = 1.2$ and $\alpha = 0.5$, corresponding to $1 - \alpha\beta g'(b^*) = 0.5833 > 0$ and $f(\beta g(0)) - 1 - rq(\beta g(0)) = -0.0867 < 0$, the traveling wave profile is monotonic. Whilst, in Fig. 8 we see non-monotonic traveling wave profiles with $1 - \alpha\beta g'(b^*) = 0.8883 > 0$ and $f(\beta g(0)) - 1 - rq(\beta g(0)) = -0.0867 < 0$. Similarly, non-monotonic wave solutions are observed in Fig. 9 even when $f(\beta g(0)) - 1 - rq(\beta g(0)) = 0.3836 \not< 0$ and with $f(\beta g(0)) - 1 - sp(\beta g(0)) - rq(\beta g(0)) = -0.6280 < 0$.

In Fig. 10, we perform simulations to assess the effect of parameters on the wave speed. It is observed that the minimal wave speed increases as β and s increase, but decreases as r increases. On the other hand, the ratio of diffusivity coefficients, d_c, does not have an effect on the traveling wave speed.

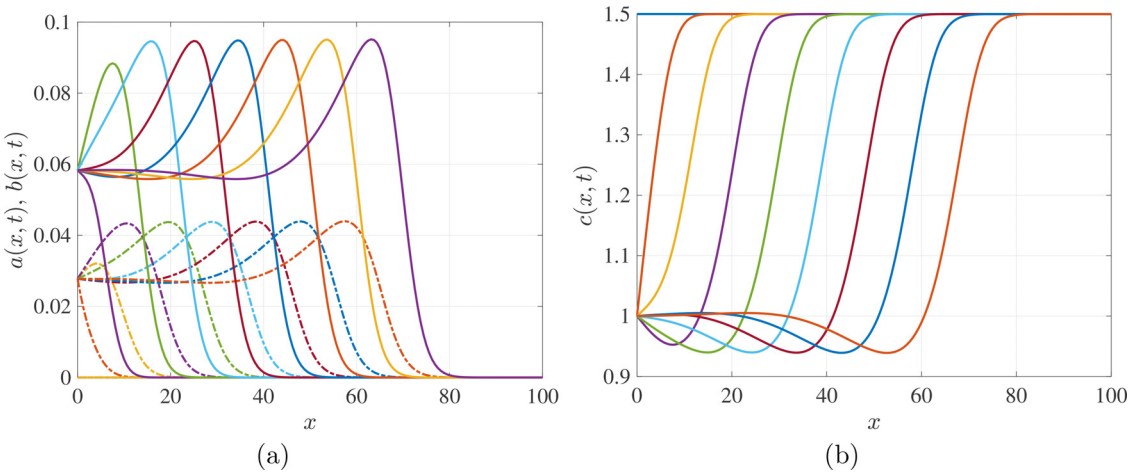

Fig. 9. Solution profiles at equally spaced intervals of 7.5 time units for $\beta = 1.5$ and $\alpha = 0.1$. In (a), the solid line denotes density b and the broken line denotes density a.

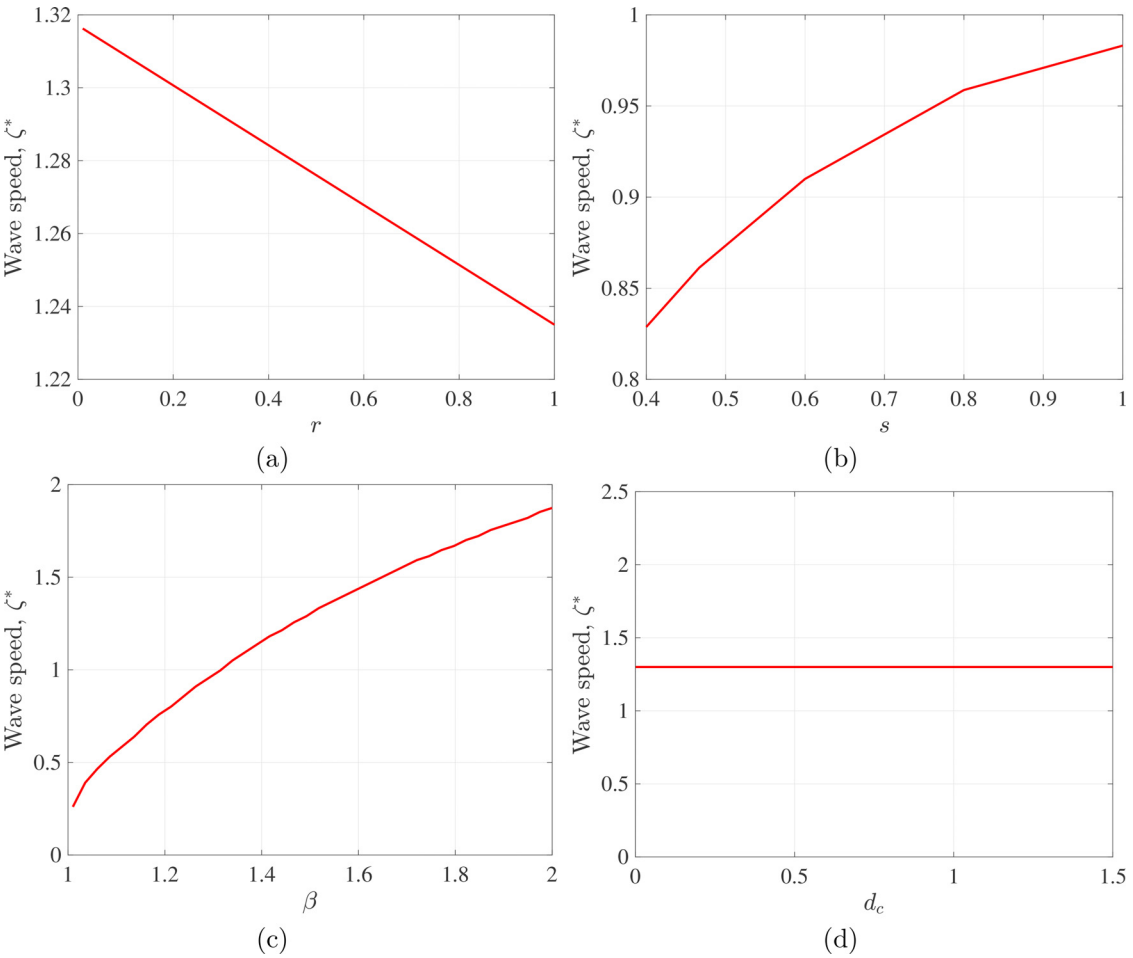

Fig. 10. The dependence of the minimal wave speed, ζ^*, on the parameters r, s, β and d_c.

6. Conclusions

Dormancy is a strategy used by microorganisms to cope with unfavorable environmental conditions. Typical models would normally ignore dormancy leading to notable model deficiencies. In practice, only a fraction of the population is active at any particular given time. In this work, we present and analyse a reaction-diffusion model that includes microbial population dormancy. Results for a uniform steady-state model predicted non-transient population oscillation when both switch functions are dependent on active microbial population density. Clearly, as discussed in Remark 5.3 of Section 5.1, disregarding the dormant state does not lead to observed oscillations in the bacterioplankton population. Furthermore, the presented reaction-diffusion model predicted that the population gradually dies out if the nutrient supply is below some threshold value and that is referred to a population under starvation. Whilst, if the nutrient levels remain above some critical value, the population is sustained in an environment as illustrated and numerically shown in Sections 3 and 5.1. Thus, the nutrient has a high impact on the composition of the population. We have shown that reaction-diffusion system of equations admits the minimal wave speed. In Section 4, we show that the traveling wave is strongly dependent on the nutrient production and the switching rates. In particular, in Section 5.2 we numerically observed a decrease in wave speed with respect to an increase in hibernation rate r. On contrary, the spreading speed increases with an increase in the awakening ratse s. Deactivation and reactivation are complex processes. These results are theoretical predictions, thus, there is still a need for experiments to test these hypotheses. Future work will include the investigation of pattern formation in these communities.

Data availability

No data was used for the research described in the article.

Acknowledgements

The authors acknowledge the support of the South African DSI-NRF SARChI Chair in Mathematical Models and Methods in Bioengineering and Biosciences. The authors wish to thank Maplesoft for providing a complimentary copy of the mathematical software Maple™, which was used in this research. Maple is a trademark of Waterloo Maple Inc. The authors are grateful to the anonymous reviewers for excellent suggestions and comments that have greatly contributed to improve the manuscript.

References

[1] E. DeLong, Microbial population genomics and ecology, Curr. Opin. Microbiol. 5 (5) (2002) 520–524.
[2] M. Gyllenberg, G. Webb, Age-size structure in populations with quiescence, Math. Biosci. 86 (1) (1987) 67–95.
[3] S. Jones, J. Lennon, Dormancy contributes to the maintenance of microbial diversity, Proc. Natl. Acad. Sci. USA 107 (13) (2010) 5881–5886.
[4] A. Kaprelyants, J. Gottschal, D. Kell, Dormancy in non-sporulating bacteria, Federation of European Microbiological Societies 104 (3–4) (1993) 271–285.
[5] T. Hoehler, B. Jørgensen, Microbial life under extreme energy limitation, Nat. Rev. Microbiol. 11 (2) (2013) 83.
[6] K. Stolpovsky, P. Martinez-Lavanchy, H. Heipieper, P. Van Cappellen, M. Thullner, Incorporating dormancy in dynamic microbial community models, Ecol. Modell. 222 (17) (2011) 3092–3102.
[7] A. Camilli, B.L. Bassler, Bacterial small-molecule signaling pathways, Science 311 (5764) (2006) 1113–1116.
[8] D. López, H. Vlamakis, R. Losick, R. Kolter, Paracrine signaling in a bacterium, Genes & Development 23 (14) (2009) 1631–1638.
[9] F. Campillo, C. Lobry, Effect of population size in a predator–prey model, Ecol. Modell. 246 (2012) 1–10.
[10] A. Fowler, H. Winstanley, Microbial dormancy and boom-and-bust population dynamics under starvation stress, Theor. Popul. Biol. 120 (2018) 114–120.
[11] J.D. Murray, E.A. Stanley, D.L. Brown, On the spatial spread of rabies among foxes, Proc. Roy. Soc. Lond. B 229 (1255) (1986) 111–150.
[12] B. Dibrov, M. Livshits, M. Volkenstein, Mathematical model of immune processes: II. kinetic features of antigenantibody interrelations, J. Theor. Biol. 69 (1) (1977) 23–39.
[13] A. Fowler, Approximate solution of a model of biological immune responses incorporating delay, J. Math. Biol. 13 (1981) 23–45.
[14] A. Huppert, B. Blasius, R. Olinky, L. Stone, A model for seasonal phytoplankton blooms, J. Theor. Biol. 236 (3) (2005) 276–290.
[15] A. Goldbeter, et al., Biochemical oscillations and cellular rhythms, Biochemical Oscillations and Cellular Rhythms (1997).
[16] E. Keller, L. Segel, Model for chemotaxis, J. Theor. Biol. 30 (2) (1971) 225–234.
[17] M. Tindall, P. Maini, S. Porter, J. Armitage, Overview of mathematical approaches used to model bacterial chemotaxis II: bacterial populations, Bull. Math. Biol. 70 (6) (2008) 1570.
[18] H. Winstanley, M. Chapwanya, M. McGuinness, A. Fowler, A polymer–solvent model of biofilm growth, Proc. Roy. Soc. Lond. A 467 (2129) (2011) 1449–1467.
[19] J. Murray, Mathematical Biology II: Spatial Models and Biomedical Applications, volume 3, Springer-Verlag, Berlin Heidelberg, 2001.
[20] M. Chen, M. Fan, R. Liu, X. Wang, X. Yuan, H. Zhu, The dynamics of temperature and light on the growth of phytoplankton, J. Theor. Biol. 385 (2015) 8–19.
[21] M. Chen, M. Fan, X. Yuan, H. Zhu, Effect of seasonal changing temperature on the growth of phytoplankton, Math. Biosci. Eng. 14 (5&6) (2017) 1091.
[22] S. Levin, L. Segel, Hypothesis for origin of planktonic patchiness, Nature 259 (5545) (1976). 659–659
[23] S. Ruan, Turing instability and travelling waves in diffusive plankton models with delayed nutrient recycling, IMA J. Appl. Math. 61 (1) (1998) 15–32.
[24] A. Sapkota, Autotrophs-definition, Types and 4 Examples, 2021, (https://microbenotes.com/autotrophs/). Last accessed on October 14, 2021.
[25] T. Zhang, W. Wang, K. Wang, Minimal wave speed of a bacterial colony model, Appl. Math. Model. 40 (23–24) (2016) 10419–10436.
[26] K. Coleman, A. Fowler, A mathematical model of exoprotein production in bacteria, Math. Med. Biol. 1 (1) (1984) 77–94.
[27] W. Jäger, S. Krömker, B. Tang, Quiescence and transient growth dynamics in chemostat models, Math. Biosci. 119 (2) (1994) 225–239.
[28] T. Malik, H. Smith, A resource-based model of microbial quiescence, J. Math. Biol. 53 (2) (2006) 231–252.
[29] B. Ayati, Microbial dormancy in batch cultures as a function of substrate-dependent mortality, J. Theor. Biol. 293 (2012) 34–40.
[30] X.-Q. Zhao, W. Wang, Fisher waves in an epidemic model, Discrete Contin. Dyn. Sys. B 4 (4) (2004) 1117.
[31] C.-H. Hsu, C.-R. Yang, T.-H. Yang, T.-S. Yang, Existence of traveling wave solutions for diffusive predator–prey type systems, J. Differ. Equ. 252 (4) (2012) 3040–3075.

[32] J. Fang, X. Zhao, Monotone wavefronts for partially degenerate reaction-diffusion systems, J. Dyn. Differ. Equ. 21 (4) (2009) 663–680.
[33] R. Mickens, Nonstandard Finite Difference Models of Differential Equations, World Scientific, Singapore, 1994.
[34] R. Anguelov, T. Berge, M. Chapwanya, J. Djoko, P. Kama, J.-S. Lubuma, Y. Terefe, Nonstandard finite difference method revisited and application to the ebola virus disease transmission dynamics, J. Differ. Equ. Appl. 26 (6) (2020) 818–854.
[35] R. Anguelov, J.-S. Lubuma, M. Shillor, Topological dynamic consistency of non-standard finite difference schemes for dynamical systems, J. Differ. Equ. Appl. 17 (12) (2011) 1769–1791.
[36] R. Anguelov, Y. Dumont, J.-S. Lubuma, M. Shillor, Dynamically consistent nonstandard finite difference schemes for epidemiological models, J. Comput. Appl. Math. 255 (2014) 161–182.